Journal of Physics: Conference Series

Effect of Yb_2O_3 stabilizing impurity on the structure and properties of $(ZrO_2)_{0.9-x}$ $(Sc_2O_3)_{0.1}(Yb_2O_3)_x$ crystals

Journal of Physics: Conference Series **1347** (2019) 012039 doi:10.1088/1742-6596/1347/1/012039

Effect of Yb_2O_3 stabilizing impurity on the structure and properties of $(ZrO_2)_{0.9-x}(Sc_2O_3)_{0.1}(Yb_2O_3)_x$ crystals

A V Kulebyakin[1], D A Agarkov[1,2], M A Borik[1], G M Eliseeva[2], V A Kolotygin[2], I E Kuritsyna[1,2], E E Lomonova[1], F O Milovich[3], V A Myzina[1], V V Osiko[1], A S Chislov[1,3] and N Yu Tabachkova[1,3]

[1]Prokhorov General Physics Institute RAS, 119991, Vavilova st. 38, Moscow, Russia
[2]Institute of Solid State Physics RAS, 142432, Academician Osipyan str. 2, Chernogolovka, Moscow region, Russia
[3]National University of Science and Technology (MISIS), 119049, Leninsky pr. 4, Moscow, Russia

e-mail: kulebyakin@lst.gpi.ru

Abstract. The effect of introduction of 0.5 – 2 mol.% Yb_2O_3 additional doping oxide into ZrO_2 – 10 mol.% Sc_2O_3 solid solutions on the phase composition, structure and electrophysical properties has been studied. ZrO_2 stabilization due to the joint effect of 10 mol.% Sc_2O_3 and 2 mol.% Yb_2O_3 provides for the formation of transparent homogeneous crystals with a cubic structure having high phase stability. Mechanical grinding of the crystals has not changed their phase composition, the powders retaining the initial fluorite crystalline structure. We show that the high-temperature electrical conductivity of the crystals decreases with an increase in the Yb_2O_3 concentration.

1. Introduction

The introduction of stabilizing scandia into zirconia based solid electrolytes produces materials having high ionic conductivity. Electrolyte membranes made from these materials provide for a significant reduction in the operation temperature of electrochemical devices while retaining the high electrical conductivity which is of great importance for increasing the service life and reliability of electrochemical reactors, solid oxide fuel cells, electrolysis cells and sensors [1-5].

According to different authors, ZrO_2 – (9-10) mol.% Sc_2O_3 ceramic has the highest ionic conductivity [6-10]. Literary data on the phase limits for zirconia stabilization with scandia differ due to the existence of metastable phases in this system making the phase composition dependent on the synthesis method and conditions. It was reported [11] that the rhombohedral phase already coexists with the cubic one at room temperature above 9.5 mol.% Sc_2O_3. The rhombohedral phase has a low electrical conductivity compared with that of the cubic phase. Upon heating the rhombohedral phase transforms to the cubic one at 400 – 600 °C. There are indications [1, 2] that additional doping of ZrO_2-Sc_2O_3 solid solutions with yttria and ceria provides for more stable cubic solid solutions with a high electrical conductivity.

Unlike ceramics, growth of single crystals allows avoiding the dependence of the electrophysical parameters on such factors as grain size, distribution of solid solution components in grain bulk and on grain boundaries, intergrain stresses and change in these parameters at high temperatures that are close to the operation temperatures of fuel cells. Study of the transport parameters of scandia stabilized

zirconia single crystals showed that the crystals having the 10 mol.% Sc_2O_3 composition had the highest electrical conductivity [12]. However, the crystals contained the rhombohedral phase along with the cubic one.

The aim of this work is to obtain single-phase cubic crystals containing 10 mol.% Sc_2O_3 by additional ytterbia doping and to assess the effect of ytterbia concentration on the phase composition, structure and physicochemical properties of the crystals, as well as the transport parameters.

2. Experimental

Solid solution single crystals were grown using directional melt crystallization in cold container in a Kristall-407 growth chamber, the cold container diameter being 130 mm and the growth rate being 10 mm/h. The weight of the molten material was 4-5 kg, the crystallization rate was 10 mm/h, and the crystallized melt ingot cooling rate was 180 to 2000 °C/min from the melt temperature (~3000 °C) to 1000 °C and 180 to 250 °C/min further to room temperature. The Yb_2O_3 content in the charge varied from 0.5 to 2 mol.% at a constant Sc_2O_3 content of 10 mol.%. The charge was produced from zirconia, scandia and ytterbia powders with at least a 99.99% purity.

The chemical composition of the crystals was studied using energy dispersion method under a JEOL 5910 LV scanning electron microscope. The phase composition of the specimens was analyzed using Raman spectroscopy on a RenishawinVia microscopic spectrometer and X-ray diffraction on a BrukerD8 diffractometer in CuKα radiation. The structure of the crystals was characterized using transmission electron microscopy under a JEM 2100 microscope at a 200 kV acceleration voltage. The specimen was thinned by ion beam etching on a PIPSII instrument.

The density of the crystals was determined using hydrostatic weighing. The microhardness and fracture toughness of the crystals were studied using the indentation method by DM 8 B AUTO driven microhardness tester with a tetrahedral Vickers pyramid.

The transport parameters of the crystals were studied in the 450 – 900 °C range with a 50 °C step using a SolartronSI 1260 analyzer at 1 Hz – 5 MHz frequencies. The test crystal wafers were 7x7 mm^2 and 0.5 mm thick with symmetrically arranged platinum electrodes produced by annealing preliminarily deposited platinum paste at 950 °C in air. The specimens were AC biased at a 24 mV amplitude. The impedance frequency spectrum was analyzed in detail with the ZView software. The electrolyte resistivity was calculated from the resultant impedance spectra, and the electrical conductivity of the crystals was then calculated.

3. Results and Discussion

ZrO_2 crystals stabilized with 10 mol.% Sc_2O_3 and additionally doped with 0.5 – 2 mol.% Yb_2O_3 were grown using directional melt crystallization in cold container. The compositions, notations, densities, microhardness and fracture toughness of the crystals are summarized in table 1 and their appearance is shown in figure 1. The crystals were 6 to 15 mm in cross-section, their length being 20 to 45 mm. The 10Sc0.5YbSZ crystals were opaque and contained no cracks (figure 1a). For addition of 1 mol.% Yb_2O_3 the crystals were semitransparent and opalescent and only their top parts contained discrete small transparent regions (figure 1b). An increase in the Yb_2O_3 content to 2 mol.% produced transparent and homogeneous single crystals (figure 1c). Analysis of the appearance of the crystals provides additional qualitative information on their phase composition (i.e. whether a crystal is a single-phase one or contains multiple phases). The presence of multiple phases or structural defects may cause light scattering at the defects or phase boundaries making the crystal opalescent or semitransparent.

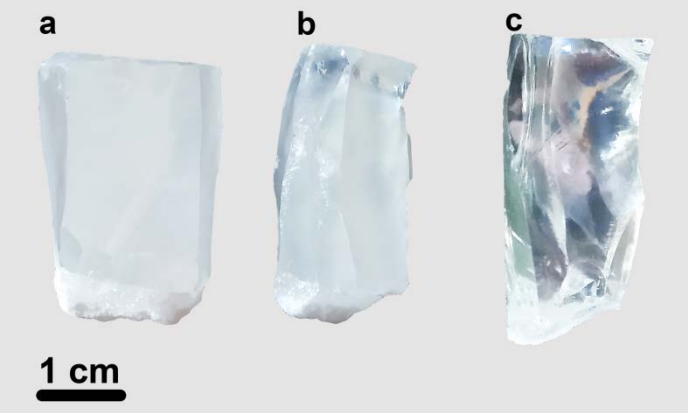

Figure 1. Appearance of crystals: (a) 10Sc0.5YbSZ; (b) 10Sc1YbSZ and (c) 10Sc2YbSZ.

With an increase in the Yb_2O_3 concentration the density of the crystals increase since ytterbia has a specific weight of 9.17 g/cm^3 which is greater than that of Sc_2O_3 (3.86 g/cm^3) и ZrO_2 (5.68 g/cm^3). In addition the density of the crystals depends not only on the Yb_2O_3 concentration but also on the phase composition of the crystals because the density of the rhombohedral phase is lower than that of the cubic one. All the test crystals had high microhardness and low fracture toughness. The microhardness of the crystals increased with an increase in the Yb_2O_3 co-doping impurity concentration in the ZrO_2-Sc_2O_3 solid solutions. The fracture toughness of the crystals depended on the Yb_2O_3 concentration but slightly but somewhat decreased with an increase in the Yb_2O_3 concentration.

Table 1. Compositions, notations, densities, microhardness and fracture toughness of crystals.

Crystal Composition	Notation	ρ, g/cm^3	HV, kg/mm^2	K_{1c}, MPa·m$^{1/2}$
$(ZrO_2)_{0.895}(Sc_2O_3)_{0.1}(Yb_2O_3)_{0.005}$	10Sc0.5YbSZ	5.793±0.001	1660 ± 30	2.6± 0.2
$(ZrO_2)_{0.89}(Sc_2O_3)_{0.1}(Yb_2O_3)_{0.01}$	10Sc1YbSZ	5.820±0.001	1735 ± 30	2.4± 0.2
$(ZrO_2)_{0.88}(Sc_2O_3)_{0.1}(Yb_2O_3)_{0.02}$	10Sc2YbSZ	5.867±0.001	1765 ± 30	2.0± 0.2

Analysis of the Sc_2O_3 and Yb_2O_3 distribution in the length of the crystals showed that the composition of all the test specimens is homogeneous, the Sc_2O_3 and Yb_2O_3 concentrations being almost the same as in the charge.

The phase composition was studied using X-ray diffraction for crystals and powders made from them (table 2). The specimens were powdered for assessing the stability of the crystal phases against mechanical impact.

Table 2. Phase composition of $(ZrO_2)_{0.9-x}(Sc_2O_3)_{0.1}(Yb_2O_3)_x$ crystals and powdered solid solutions (x = 0.005 – 0.02).

Specimen	Phase composition	Lattice parameter	
		a, nm	c, nm
$(ZrO_2)_{0.9-x}(Sc_2O_3)_{0.1}(Yb_2O_3)_y$ crystals			
10Sc0.5YbSZ	c – ZrO_2	0.5095 (1)	
	r – ZrO_2	0.3559 (5)	0.9005(5)
10Sc1YbSZ	c – ZrO_2	0.5095(1)	
	r – ZrO_2	0.3563 (2)	0.9003(2)
10Sc2YbSZ	c – ZrO_2	0.5096(1)	
$(ZrO_2)_{0.9-x}(Sc_2O_3)_{0.1}(Yb_2O_3)_y$ powders			
10Sc0.5YbSZ	r – ZrO_2	0.3560 (5)	0.9004(5)
10Sc1YbSZ	r – ZrO_2	0.3565 (2)	0.9002(2)
10Sc2YbSZ	c – ZrO_2	0.5096(1)	

The phase composition of the crystals changed with an increase in the Yb_2O_3 concentration. The ZrO_2 crystals stabilized with 10 mol.% Sc_2O_3 and additionally doped with 0.5 and 1 mol.% Yb_2O_3 were mixtures of the rhombohedral and cubic ZrO_2 modifications. However the cubic phase in the crystals is unstable and transformed completely to the rhombohedral phase as a result of grinding. The 10Sc2YbSZ crystals contained only the cubic ZrO_2 modification and did not undergo the abovementioned phase transition during grinding: the crystals retained their initial fluorite structure.

The phase composition of the crystals was also analyzed using Raman spectroscopy (figure 2). The Raman spectra of the 10Sc0.5YbSZ and 10Sc1YbSZ crystals contain only the rhombohedral phase peaks that are quite broadened which may indicate the presence of the cubic phase. The peak positions for the 10Sc2YbSZ crystals coincide with those typical of the cubic phase.

Thus, phase analysis suggests that the cubic phase can only be stabilized in the ZrO_2–10 mol.% Sc_2O_3 crystals by co-doping with 2 mol.% Yb_2O_3.

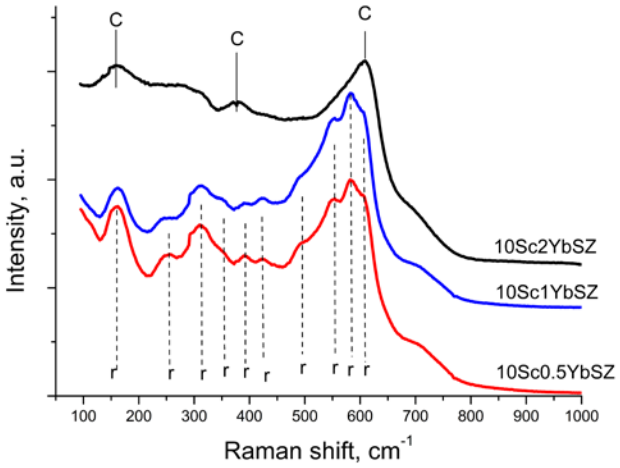

Figure 2. Raman spectra of 10Sc0.5YbSZ, 10Sc1YbSZ and 10Sc2YbSZ crystals.

Transmission electron microscopy study showed that the 10Sc0.5YbSZ and 10Sc1YbSZ contain twins. Figure 3 (a, b) shows that the primary twinning plates of the crystals also undergo twinning. The traces of the secondary twinning planes are at ~ 90 arc deg to the trace of the primary twinning plane. Twinning during the rhombohedral-cubic transition in the 10Sc0.5YbSZ and 10Sc1YbSZ crystals is similar to that in ZrO_2–Y_2O_3 ones [13]. The cubic 10Sc2YbSZ crystals contain no twins (figure 3c).

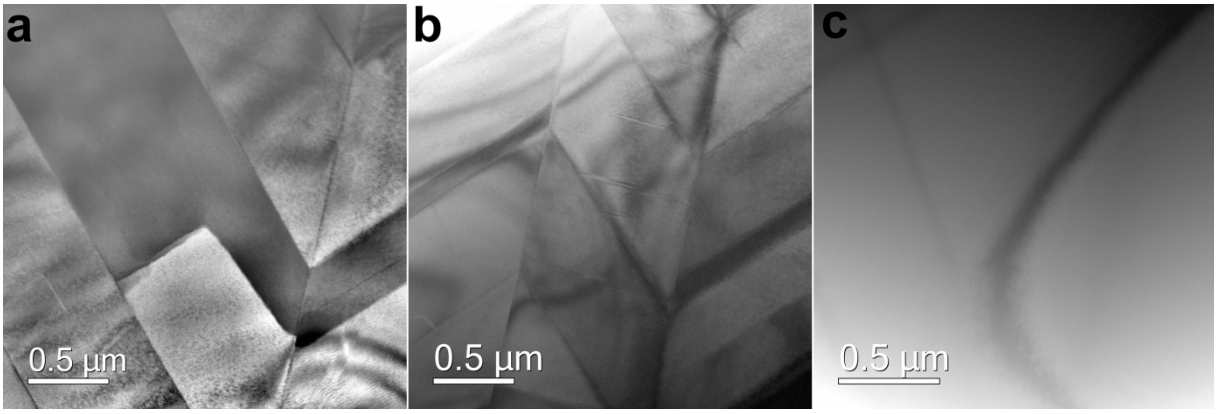

Figure 3. TEM images of crystal structure: (a) 10Sc0.5YbSZ; (b) 10Sc1YbSZ; (c) 10Sc2YbSZ.

Figure 4 (a) shows the electrical conductivity of the crystals as a function of temperature in Arrhenius coordinates. It can well be seen that the electrical conductivities of the 10Sc0.5YbSZ and

10Sc1YbSZ crystals are close in almost the entire test temperature range. The temperature dependences of the electrical conductivity of the 10Sc0.5YbSZ and 10Sc1YbSZ crystals exhibits a conductivity discontinuity caused by the rhombohedral-cubic transition. The electrical conductivity of the 10Sc1YbSZ crystals is higher than that of the 10Sc0.5YbSZ ones in the phase transition temperature range since the 10Sc1YbSZ crystals contain less rhonbohedral phase which reduces the electrical conductivity. The single-phase cubic 10Sc2YbSZ single crystals do not exhibit an electrical conductivity discontinuity in the temperature dependences of the electrical conductivity, the electrical conductivity of the 10Sc2YbSZ crystals being higher than those of the 10Sc0.5YbSZ and 10Sc1YbSZ crystals in the phase transition temperature range. Figure 4 (b) shows the electrical conductivities of the crystals at different temperatures. It can be seen that the electrical conductivity of the crystal decreases with an increase in the ytterbia concentration at high temperatures (700–900 °C).

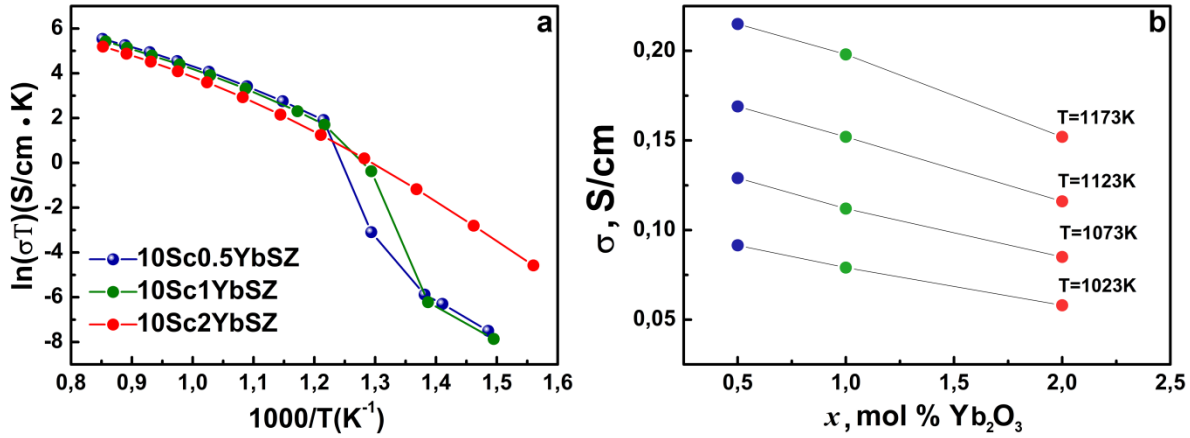

Figure 4. Electrical conductivity of crystals (a) as a function of temperature and (b) Yb_2O_3 concentration.

The data summarized in table 3 show that the high temperature activation energy is the lowest for the 10Sc0.5YbSZ crystals (0.72 eV) and the highest for the 10Sc2YbSZ crystals (0.81 eV), i.e., the carrier mobility decreases with an increase in the Yb_2O_3 concentration. This agrees with studies of ceramics [5, 14] showing that an increase in the stabilizing impurity concentration reduces the electrical conductivity, this phenomenon being attributed to a decrease in the carrier mobility due to the larger ionic radius of the stabilizing oxide.

Table 3. Activation energy of $(ZrO_2)_{0.9-x}(Sc_2O_3)_{0.1}(Yb_2O_3)_x$ crystals (x = 0.005 – 0.02) in the 673–1173 K range.

Specimen	Activation energy E_a, eV	
	673 K – 823 K	823 K – 1173 K
10Sc0.5YbSZ	1.33	0.72
10Sc1YbSZ	1.31	0.76
10Sc2YbSZ	1.48	0.81

4. Conclusions

$(ZrO_2)_{0.9-x}(Sc_2O_3)_{0,1}(Yb_2O_3)_x$ solid solution crystals (x = 0.005 – 0.02) were grown using directional melt crystallization. Stabilization with 10 mol.% Sc_2O_3 and 2 mol.% Yb_2O_3 doping impurities provides for transparent and homogeneous ZrO_2 crystals with a cubic structure.

Analysis of scandia and yttria distributions in the length of the crystals showed that the composition of all the test specimens is homogeneous, the Sc_2O_3 and Yb_2O_3 concentrations being almost the same as in the charge. Comparison of the phase composition data for the crystals and the

powders showed that the 10Sc2YbSZ crystals have high phase stability: mechanical grinding did not change the phase composition of the crystals.

An increase in the Yb_2O_3 content in the solid electrolyte to 2 mol.% reduces the high-temperature electrical conductivity of the 10Sc2YbSZ crystals compared with those of the 10Sc0.5YbSZ and 10Sc1YbSZ crystals due to a decrease in the carrier mobility with an increase in the stabilizing oxide concentration.

Acknowledgments
This work was performed with the financial support of the Russian Scientific Foundation (project № 19-72-10113).

References

[1] Badwal S P S, Ciacchi F T and Milosevic D 2000 Scandia-zirconia electrolytes for intermediate temperature solid oxide fuel cell operation *Solid State Ionics* **136–137** 91–9
[2] Kharton V V, Marques F M B and Atkinson A 2004 Transport properties of solid oxide electrolyte ceramics: a brief review *Solid State Ionics* **174** 135–49
[3] Fergus J W 2006 Electrolytes for solid oxide fuel cells *J. Power Sources* **162** 30–40
[4] Yokokawa H, Sakai N, Horita T, Yamaji K and Brito M E 2005 Solid oxide electrolytes for high temperature fuel cells *Electrochemistry* **73** 20–30
[5] Politova T I and Irvine J T S 2004 Investigation of scandia–yttria–zirconia system as an electrolyte material for intermediate temperature fuel cells—influence of yttria content in system $(Y_2O_3)_x(Sc_2O_3)_{(11-x)}(ZrO_2)_{89}$ *Solid State Ionics* **168** 153–65
[6] Wakako A, Hanashiro D, Arai Y and Malzbender J 2013 Fracture mechanism of scandia-doped zirconia *Acta Mater.* **61** 3082–9
[7] Fujimori H, Yashima M, Kakihana M and Yoshimura M 1998 Structural changes of scandia-doped zirconia solid solutions: rietveld analysis and raman scattering *J. Am. Ceram. Soc.* **81** 2285–93
[8] Simoncic P and Navrotsky A 2007 Systematics of phase transition and mixing energetics in rare earth *J. Am. Ceram. Soc.* **90** 2143–50
[9] Spirin A, Ivanov V, Nikonov A, Lipilin A, Paranin S, Khrustov V and Spirina A 2012 Scandia-stabilized zirconia doped with yttria: synthesis, properties, and ageing behavior *Solid State Ionics* **225** 448–52
[10] Tataryn T, Savytskii D, Paulmann C and Bismayer U 2009 Twin structure of the ZrO_2:Sc_2O_3 crystal *Radiat. Phys. Chem.* **78** 101–4
[11] Shobit O, Najib W B, Chen W and Bonanos N 2012 Electrical conductivity of 10 mol% Sc_2O_3 – 1 mol% M_2O_3 – ZrO_2 Ceramics *J. Am. Ceram. Soc.* **95** 1965-72
[12] Borik M A et al. 2016 Melt growth, structure and properties of $(ZrO_2)_{1-x}(Sc_2O_3)_x$ solid solution crystals (x=0.035-0.11) *J. Cryst. Growth* **443** 54-61
[13] Borik M A, Bublik V T, Kulebyakin A V, Lomonova E E, Milovich F O, Myzina V A, Osiko V V, Seryakov S V and Tabachkova N Y 2015 Change in the phase composition, structure and mechanical properties of directed melt crystallised partially stabilised zirconia crystals depending on the concentration of Y_2O_3 *J. Eur. Ceram. Soc.* **35** 1889–94
[14] Yuan F, Wang J, Miao H, Guo C and Wang W G 2013 Investigation of the crystal structure and ionic conductivity in the ternary system $(Yb_2O_3)_x$–$(Sc_2O_3)_{(0.11-x)}$–$(ZrO_2)_{0.89}$ (x = 0–0.11) *J. Alloy Compd.* **549** 200–5